

A Polynomial Neural Network with Controllable Precision and Human-Readable Topology for Prediction and System Identification

Gang Liu, Jing Wang
Xi'an Jiaotong University
{gangliu.6677, wangpele}@gmail.com

October 31, 2022

Abstract

Although artificial neural networks (ANNs) are successful, there is still a concern among many over their black box nature. Why do they work? Could we design a transparent network? This paper presents a controllable and readable polynomial neural network (CR-PNN) for approximation, prediction, and system identification. CR-PNN is simple enough to be described as one small formula, so that we can control the approximation precision and explain the internal structure of the network. CR-PNN, in fact, essentially is the fascinating Taylor expansion in the form of network. The number of layers represents precision. Derivatives in Taylor expansion are exactly imitated by error back-propagation algorithm. Firstly, we demonstrated that CR-PNN shows excellent analysis performance to the black box system through ten synthetic data with noise. Also, the results were compared with synthetic data to substantiate its search easily towards the global optimum. Secondly, it was verified, by ten real-world applications, that CR-PNN brought better generalization capability relative to the typical ANNs that approximate depended on the nonlinear activation function. Finally, 200,000 repeated experiments, with 4898 samples, demonstrated that CR-PNN is five times more efficient than typical ANN for one epoch and ten times more efficient than typical ANN for one forward-propagation. In short, compared with the traditional neural networks, the novelties and advantages of CR-PNN include readability of the internal structure, easy to find global optimal solution, lower computational complexity, and likely better robustness to real-world approximation. (We're strong believers in Open Source, and provide CR-PNN code for others. GitHub: <https://github.com/liugang1234567/CR-PNN#cr-pnn>)

1 Introduction

An artificial neural network inspired by the biological neural system has achieved great success in many fields, e.g., classification, prediction, and control [1–3]. In recent years, the structure of ANN has become deeper. Nevertheless, it has almost never been changed about the method which achieves nonlinear mapping by different nonlinear activation functions. Although this method showed an outstanding performance in a variety of problems, it makes the model look like a black-box due to the unknown nonlinear structure [4].

The unknown structure raises two challenging issues: over-fitting and falling into the local optimum. Regularization and early termination have been proved effective in terms of solving the over-fitting [5]. Nevertheless, according to many in the field, we cannot understand the detailed changes and then achieve targeted control of precision when we tune the hyperparameters [5]. In the aspect of searching for the global optimum, some optimization algorithms have been used, such as the genetic algorithm and simulate anneal algorithm [6, 7]. However, typically, such algorithms do not search the entire solution space, and they cannot ensure to find a globally optimal solution.

In this paper, we attempt to design a transparent network without nonlinear activation functions where we could explain the internal nonlinear structure of the network while keeping the excellent approximation property of ANN. Understanding the internal structure of the network is vitally important, which will help us search for the global optimum better, achieve targeted design for different problems, and analyze unknown systems.

In 2018, Norman Matloff et al. showed an interesting work [8]. They demonstrated the existing ANNs are, in fact, essentially polynomial regression models (PR), with the effective degree of the polynomial growing at each hidden layer.

Without a doubt, polynomial mappings may approximate any continuous real function from the input space to the output space to any required degree of accuracy [9]. A typical example is Taylor expansion. We can get the required degree of accuracy by controlling the highest order term. Here, we will apply this good idea to ANN.

The rest of this paper is organized as follows. Section II describes the network structure of CR-PNN. The learning rules of CR-PNN is provided in Section III. Section IV shows the system identification capability of CR-PNN. In Section V, we explore the generalization capability and computational complexity of CR-PNN and discuss some other likely noteworthy details. Section VI provides the concluding remarks of the paper. Besides, in this paper, we use the term ANN to mean general feedforward networks such as back-propagation neural networks (BPNN), as opposed to specialized models such as convolutional neural networks (CNNs) for image classification and recurrent neural networks (RNNs) for text processing [10].

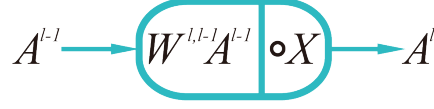


Figure 1: Single-layer structure of CR-PNN.

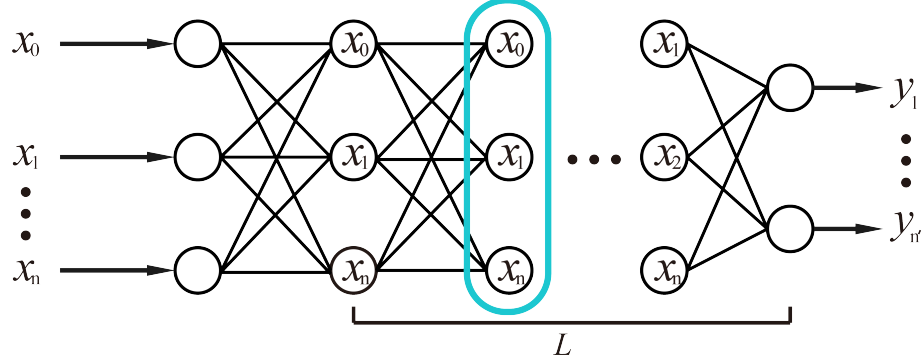


Figure 2: Overall structure of CR-PNN.

2 Network structure of CR-PNN

The overall structure of CR-PNN is shown in Fig. 2. The overall structure can be represented according to the following formula:

$$f(X) = W^{L,L-1}[\dots W^{l,l-1}(\dots W^{21}(W^{10}X \circ X) \circ X \dots) \circ X \dots], L \in N+ \quad (1)$$

Where X and $Y = f(X)$ denotes the input space and the output space. $W^{l,l-1}$ is the weight matrix from the $l-1$ -th layer to the l -th layer. Also, x_0 in X is equal to 1, which tune the bias. It should be noted that L expresses the number of hidden layers plus the output layer and represents the highest item of the network similar to Taylor expansion. Additionally, it is well known that the computational complexity of hadamard product is significantly lower than nonlinear functions, such as tansig. The single-layer structure of CR-PNN is straightforward (see Fig. 1). The output of the current layer A^l is defined as

$$A^l = W^{l,l-1} A^{l-1} \circ X \quad (2)$$

Where A^{l-1} is the output of the previous layer.

Also, CR-PNN is, in fact, essentially the expression of multivariate Taylor expansion or Maclaurin series, according to Jiushao Qin or Horner Algorithm. Taylor and Maclaurin have demonstrated the approximation property of CR-PNN. According to Taylor expansion, the coefficients of the Taylor series that are represented by the weight matrix W are the optimal solution.

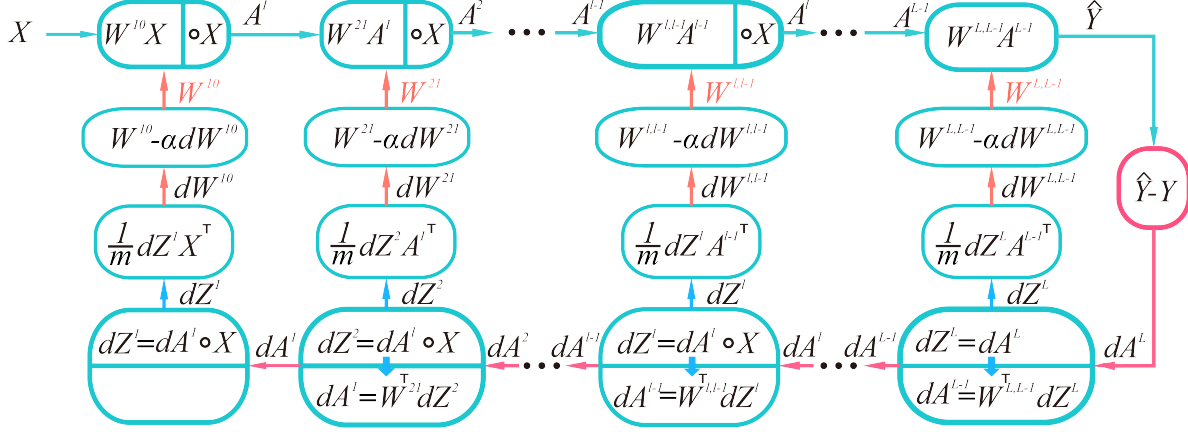


Figure 3: Graphical illustration of learning rules.

3 Learning Rules of CR-PNN

The graphical illustration of learning rules is shown in Fig. 3. We describe an error back-propagation based learning rule for CR-PNN [11]. The simplicity of the learning method makes it convenient for the model to be used in different situations. Additionally, the weight of the higher layer of CR-PNN has a more significant impact on the coefficients of the lower items. The learning rules can also be interpreted that the outline of output space is fitted by lower item, and later the higher item modifies the details. The following set of equations describes the simple gradient descent rule.

The forward-propagation of hidden layers and output layer:

$$\begin{cases} A^l = W^{l,l-1} A^{l-1} \circ X \\ A^L = W^{L,L-1} A^{L-1} \end{cases} \quad (3)$$

The error-backpropagation of output layer and hidden layers:

$$dA^L = \hat{Y} - Y \quad (4)$$

$$\begin{cases} dZ^L = dA^L \\ dZ^l = dA^l \circ X \end{cases} \quad (5)$$

$$dA^{l-1} = (W^{l,l-1})^T dZ^l \quad (6)$$

The weight adjustment of the network:

$$dW^{l,l-1} = \frac{1}{m} dZ^l (A^{l-1})^T \quad (7)$$

$$W^{l,l-1(new)} = W^{l,l-1(old)} - \alpha dW^{l,l-1} \quad (8)$$

Where \hat{Y} and Y is the output of network and label, respectively. n denotes the number of training samples in one batch. The learning rate can either be adapted with epochs or can be fixed to a small number based on heuristics.

This learning method is used to train CR-PNN in the next section to solve some famous problems relating to system identification [12] and function approximation [13]. Interestingly, we may solve the Taylor series or some order derivative at zero for the function that cannot be represented by the formula.

4 System identification with CR-PNN

Unlike the typical neural networks that approximate depend on the nonlinear activation function, the network proposed in this paper can be translated into the form of polynomials. Thus, this advantage allows it to be applied for system identification. To evaluate its performance for system identification, we performed a set of experiments with synthetic data. The experiments are carried out using MATLAB 2019b. For quantitative analysis, we employ the commonly used mean squared error (MSE) as the measurement of performance [14].

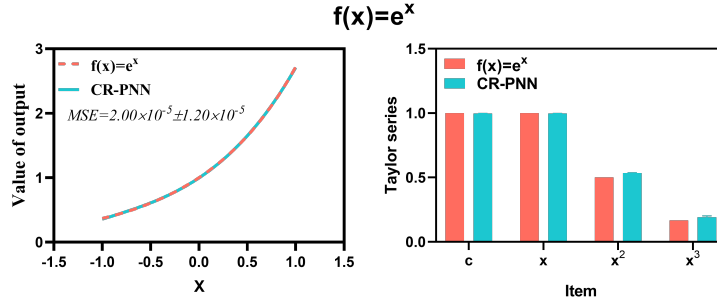
4.1 Identification of Taylor expansion

As an example, we select three-layers CR-PNN with two inputs and one output. This means that the network is a third-order polynomial, and is described by the following equation:

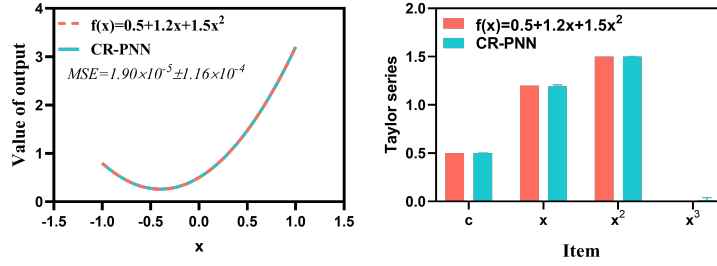
$$\begin{aligned}
f(X) &= W^{32}(W^{21}((W^{10}X) \circ X) \circ X) \\
&= W^{32}\left(W^{21}\left(\begin{bmatrix} w_{11}^{10} & w_{12}^{10} \\ w_{21}^{10} & w_{22}^{10} \end{bmatrix} \begin{bmatrix} x_0 \\ x_1 \end{bmatrix} \circ \begin{bmatrix} x_0 \\ x_1 \end{bmatrix}\right) \circ X\right) \\
&= W^{32}\left(\begin{bmatrix} w_{11}^{21} & w_{12}^{21} \\ w_{21}^{21} & w_{22}^{21} \end{bmatrix} \begin{bmatrix} w_{11}^{10}x_0^2 + w_{12}^{10}x_0x_1 \\ w_{21}^{10}x_0x_1 + w_{22}^{10}x_1^2 \end{bmatrix} \circ \begin{bmatrix} x_0 \\ x_1 \end{bmatrix}\right) \\
&= \begin{bmatrix} w_{11}^{32} & w_{12}^{32} \end{bmatrix} \begin{bmatrix} w_{11}^{10}w_{11}^{21}x_0^3 + (w_{12}^{10}w_{11}^{21} + w_{21}^{10}w_{12}^{21})x_0^2x_1 + w_{22}^{10}w_{12}^{21}x_0x_1^2 \\ w_{11}^{10}w_{21}^{21}x_0^2x_1 + (w_{12}^{10}w_{21}^{21} + w_{21}^{10}w_{22}^{21})x_0x_1^2 + w_{22}^{10}w_{22}^{21}x_1^3 \end{bmatrix} \\
&= w_{11}^{10}w_{11}^{21}w_{11}^{32}x_0^3 + w_{22}^{10}w_{22}^{21}w_{12}^{32}x_1^3 \\
&\quad + (w_{12}^{10}w_{11}^{21}w_{11}^{32} + w_{21}^{10}w_{12}^{21}w_{11}^{32} + w_{11}^{10}w_{21}^{21}w_{12}^{32})x_0^2x_1 \\
&\quad + (w_{22}^{10}w_{12}^{21}w_{11}^{32} + w_{12}^{10}w_{21}^{21}w_{12}^{32} + w_{21}^{10}w_{22}^{21}w_{12}^{32})x_0x_1^2
\end{aligned} \tag{9}$$

Where x_0 is equal to 1. Thus, the output of this network is consist of constant c , x_1^3 , x_1 , and x_1^2 items. The exact form of the polynomials is specific to the topology of CR-PNN, and coefficients are in terms of the weights of the network.

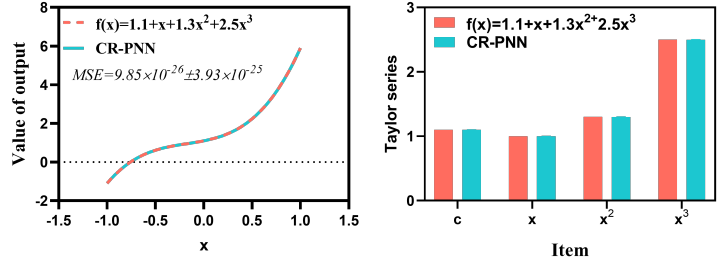
To test whether CR-RNN happens to be a three-order Taylor expansion, we selected $f(x) = e^x$ for an example. Also, we compared the output of the network with corresponding two-order, three-order, and four-order functions to explore the influence on the model when redundancy and inadequacy of the number of layers of the designed network. For a more comprehensive comparison, we run



The highest item of systems:2



The highest item of systems:3



The highest item of systems:4

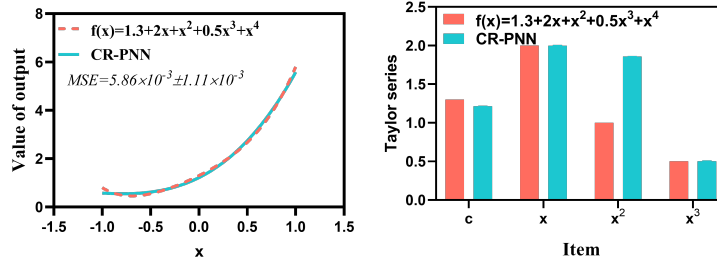


Figure 4: Identification of Taylor expansion. All the networks for 200 runs with different initial parameters.

the algorithms 200 times using 200 different initial parameters for each CR-RNN model, as shown in Fig. 4. These results indicate that three attractive property of CR-PNN:

1) The CR-RNN happens to be a Taylor expansion. Also, by using experiments, this paper has successfully demonstrated Taylor expansion is the optimal decomposition form for approximating continuous real function using a polynomial. This means the structure of the network has visualized significance, and the network maybe is practical tools to solve the Taylor expansion for functions that cannot be represented by the formula.

2) The networks can easily converge to the global optimum, as evidenced by 200 runs using 200 different initial parameters.

3) When layers of the designed network are inadequate, CR-PNN will try to search for the global optimum weights to approach the labels.

4.2 Identification via the approximation property of CR-PNN

For an unknown system, we should tune numbers of layers of networks to simulate the real system, and then translate the network into polynomial among input and output space. In order to investigate the approximation property of CR-PNN, we consider the function fitting of the normalized Bessel function defined by:

$$f(x) = \frac{\sin(x)}{x^2} - \frac{\cos(x)}{x^2} \quad (10)$$

Where we defined $x \in [-10, 0) \cup (0, 10]$, then x and $f(x)$ is normalized to $[-1, 1]$, respectively.

We gradually increase the number of layers to approach the normalized Bessel function. All the networks run 200 times with different initial parameters (see Fig. 5). In this experiment, the accuracy increased from layer to layer. This increasing property corresponds to the property in Taylor expansion, as expected under the formula.

4.3 Identification of multiple-input system with noise

As an example, we select three-layers CR-PNN with three inputs and one output. The network is described by the following equation:

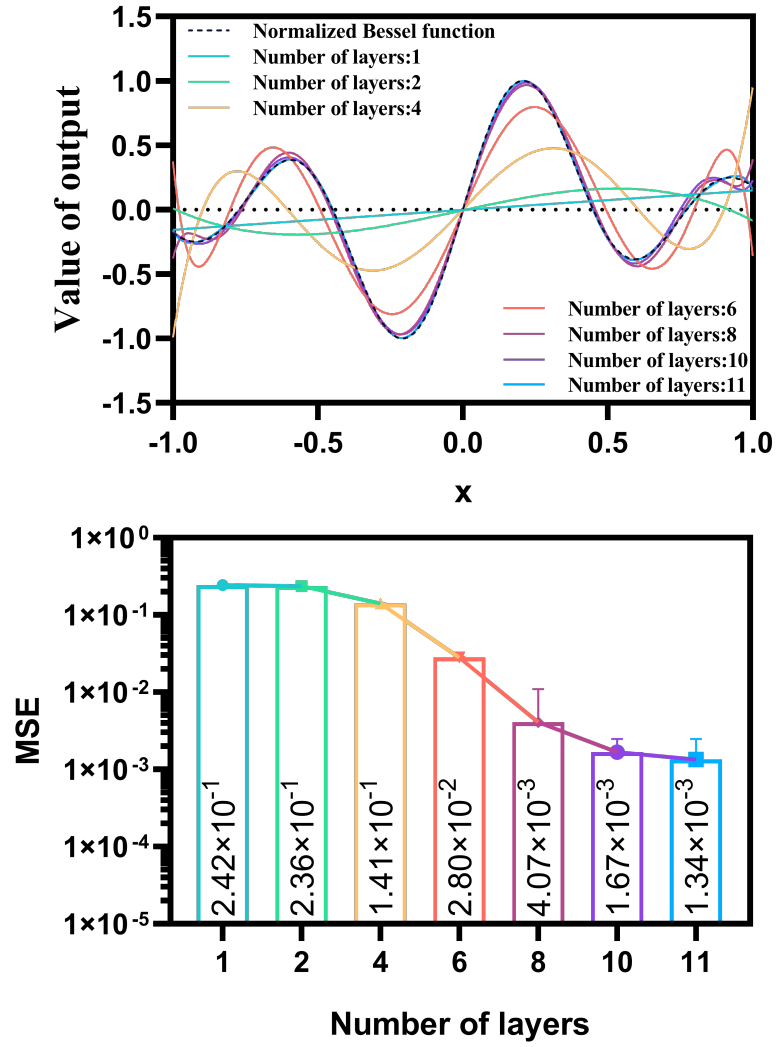


Figure 5: Approximation of normalized Bessel function. All the networks for 200 runs with different initial parameters.

$$\begin{aligned}
f(X) &= W^{32}(W^{21}((W^{10}X) \circ X) \circ X) \\
&= W^{32}\left(W^{21}\left(\begin{bmatrix} w_{11}^{10} & w_{12}^{10} & w_{13}^{10} \\ w_{21}^{10} & w_{22}^{10} & w_{23}^{10} \\ w_{31}^{10} & w_{32}^{10} & w_{33}^{10} \end{bmatrix} \begin{bmatrix} x_0 \\ x_1 \\ x_2 \end{bmatrix} \circ \begin{bmatrix} x_0 \\ x_1 \\ x_2 \end{bmatrix}\right) \circ X\right) \\
&= W^{32}\left(\begin{bmatrix} w_{11}^{21} & w_{12}^{21} & w_{13}^{21} \\ w_{21}^{21} & w_{22}^{21} & w_{23}^{21} \\ w_{31}^{21} & w_{32}^{21} & w_{33}^{21} \end{bmatrix} \begin{bmatrix} w_{11}^{10}x_0^2 + w_{12}^{10}x_0x_1 + w_{13}^{10}x_0x_2 \\ w_{21}^{10}x_0x_1 + w_{22}^{10}x_1^2 + w_{23}^{10}x_1x_2 \\ w_{31}^{10}x_0x_2 + w_{32}^{10}x_1x_2 + w_{33}^{10}x_2^2 \end{bmatrix} \circ \begin{bmatrix} x_0 \\ x_1 \\ x_2 \end{bmatrix}\right) \\
&= \begin{bmatrix} w_{11}^{32} & w_{12}^{32} & w_{13}^{32} \end{bmatrix} \begin{bmatrix} w_{11}^{10}w_{11}^{21}x_0^3 + (w_{12}^{10}w_{11}^{21} + w_{21}^{10}w_{12}^{21})x_0^2x_1 \\ + (w_{13}^{10}w_{11}^{21} + w_{31}^{10}w_{13}^{21})x_0^2x_2 + w_{22}^{10}w_{12}^{21}x_0x_1^2 \\ + (w_{23}^{10}w_{12}^{21} + w_{32}^{10}w_{13}^{21})x_0x_1x_2 + w_{33}^{10}w_{13}^{21}x_0x_2^2 \\ \\ w_{11}^{10}w_{21}^{21}x_0^2x_1 + (w_{12}^{10}w_{21}^{21} + w_{21}^{10}w_{22}^{21})x_0x_1^2 \\ + (w_{13}^{10}w_{21}^{21} + w_{31}^{10}w_{23}^{21})x_0x_1x_2 + w_{22}^{10}w_{22}^{21}x_1^3 \\ + (w_{23}^{10}w_{22}^{21} + w_{32}^{10}w_{23}^{21})x_1^2x_2 + w_{33}^{10}w_{23}^{21}x_1x_2^2 \\ \\ w_{11}^{10}w_{31}^{21}x_0^2x_2 + (w_{12}^{10}w_{31}^{21} + w_{21}^{10}w_{32}^{21})x_0x_1x_2 \\ + (w_{13}^{10}w_{31}^{21} + w_{31}^{10}w_{33}^{21})x_0x_2^2 + w_{22}^{10}w_{32}^{21}x_1^2x_2 \\ + (w_{23}^{10}w_{32}^{21} + w_{32}^{10}w_{33}^{21})x_1x_2^2 + w_{33}^{10}w_{33}^{21}x_2^3 \end{bmatrix} \\
&= w_{11}^{10}w_{11}^{21}w_{11}^{32}x_0^3 + w_{22}^{10}w_{22}^{21}w_{22}^{32}x_1^3 + w_{33}^{10}w_{33}^{21}w_{33}^{32}x_2^3 \\
&\quad + (w_{12}^{10}w_{11}^{21}w_{11}^{32} + w_{21}^{10}w_{12}^{21}w_{11}^{32} + w_{11}^{10}w_{21}^{21}w_{12}^{32})x_0^2x_1 \\
&\quad + (w_{13}^{10}w_{11}^{21}w_{11}^{32} + w_{31}^{10}w_{13}^{21}w_{11}^{32} + w_{11}^{10}w_{31}^{21}w_{13}^{32})x_0^2x_2 \\
&\quad + (w_{22}^{10}w_{12}^{21}w_{11}^{32} + w_{12}^{10}w_{21}^{21}w_{12}^{32} + w_{21}^{10}w_{22}^{21}w_{12}^{32})x_0x_1^2 \\
&\quad + (w_{33}^{10}w_{13}^{21}w_{11}^{32} + w_{13}^{10}w_{31}^{21}w_{13}^{32} + w_{31}^{10}w_{33}^{21}w_{13}^{32})x_0x_2^2 \\
&\quad + (w_{23}^{10}w_{22}^{21}w_{12}^{32} + w_{32}^{10}w_{23}^{21}w_{12}^{32} + w_{22}^{10}w_{32}^{21}w_{13}^{32})x_1^2x_2 \\
&\quad + (w_{33}^{10}w_{23}^{21}w_{12}^{32} + w_{23}^{10}w_{32}^{21}w_{13}^{32} + w_{32}^{10}w_{33}^{21}w_{13}^{32})x_1x_2^2 \\
&\quad + (w_{23}^{10}w_{12}^{21}w_{11}^{32} + w_{32}^{10}w_{13}^{21}w_{11}^{32} + w_{13}^{10}w_{21}^{21}w_{12}^{32}) \\
&\quad + (w_{31}^{10}w_{23}^{21}w_{12}^{32} + w_{12}^{10}w_{31}^{21}w_{13}^{32} + w_{21}^{10}w_{32}^{21}w_{13}^{32})x_0x_1x_2
\end{aligned} \tag{11}$$

Where x_0 is equal to 1. Thus, the output of this network consists of constant c , x_1^3 , x_2^3 , x_1 , x_2 , x_1^2 , x_2^2 , $x_1^2x_2$, $x_1x_2^2$, and x_1x_2 items.

In order to assess the identification performance of CR-PNN to a multiple-input system with noise, we constructed the three-order system:

$$f(u, v) = 0.1 + 0.2u + 0.3v + 0.4uv + 0.5u^2 + 0.6v^2 + 0.7u^2v + 0.8uv^2 + 0.9u^2 + v^3 \tag{12}$$

Then, we add white Gaussian noise to $f(u, v)$ to generate the output labels $F(u, v)$ of networks.

$$F(u, v) = f(u, v) + N \tag{13}$$

Where N is the Gaussian noise. We explore identification performance with a signal-to-noise ratio (SNR) of -10 , 0 , and 10 db, respectively, when the input

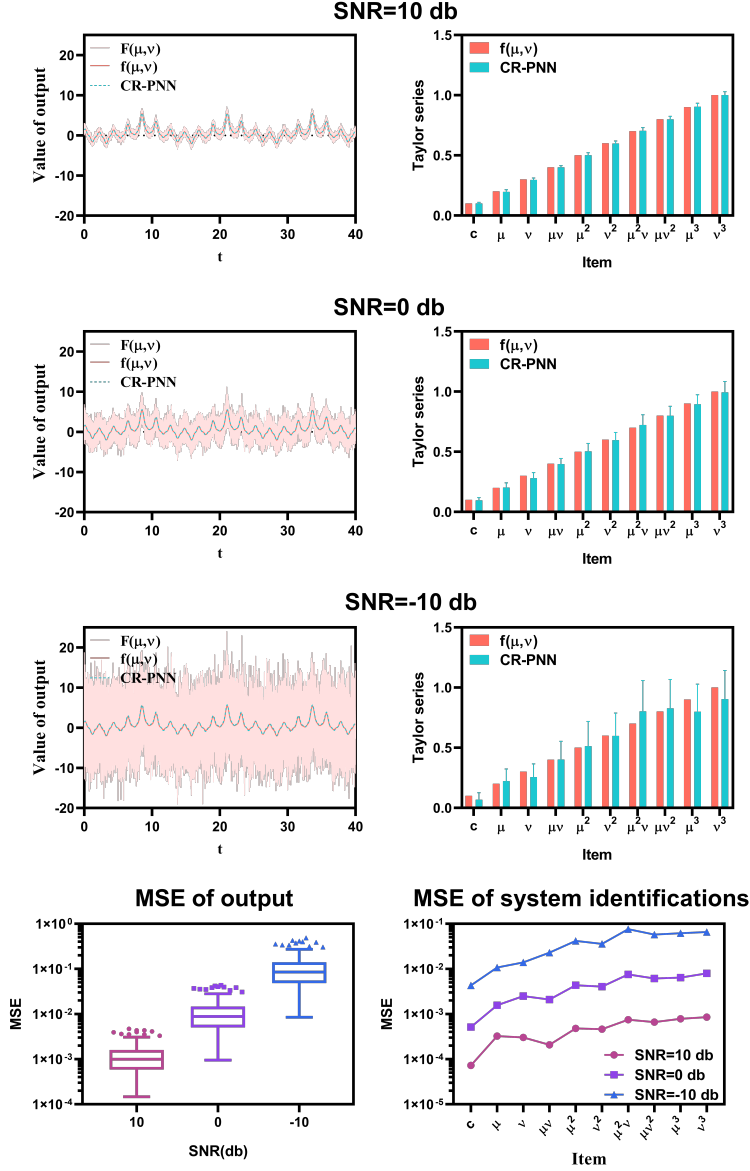


Figure 6: Identification of multiple-input system with noise. All the networks for 200 runs with different initial parameters and output labels in each case of SNR.

is defined by:

$$\begin{cases} u(t) = \sin(\frac{1}{2}t + 60) \\ v(t) = \sin(3t + 20) \end{cases} \quad (14)$$

Where we defined $t \in [0, 40]$. We run the algorithms 200 times using 200 different initial parameters and $F(u, v)$ in each case of SNR, as shown in Fig. 6. It should be noted that we should compare the network model with the three-order system $f(u, v)$ required to be identified rather than the output labels $F(u, v)$. These results indicate that two attractive properties of CR-PNN: 1) CR-PNN showed great identification performance to a multiple-input system with noise even in the case of SNR of -10 . 2) As SNR decreased, MSE of system coefficients identification and output increased. Interestingly, MSE of higher items increased greater than lower items with SNR decreased [Note that the ordinate is logarithmic coordinates in Fig. 6 (MSE)]. According to the learning rules of networks, the outline of output space is fitted by lower item, and later the higher item modifies the details, which interpreted this phenomenon.

5 Generalization capability and computational complexity of CR-PNN

Generally, a good network should have considerable generalization capability and lower computational complexity. Using ten real-world datasets obtained from different fields, we compared CR-PNN with typical neural networks in Matlab 2019b Neural Net toolbox on a 2.2-GHz laptop PC.

1) Dataset 1: Yacht Hydrodynamics [15]

Prediction of residuary resistance of sailing yachts at the initial design stage is of excellent value for evaluating the performance and for estimating the required propulsive power. The dataset comprises 308 full-scale experiments that were performed at the Delft Ship Hydromechanics Laboratory. Attribute information includes six hull geometry coefficients, the Froude number, and the residuary resistance per unit weight of displacement. In this test, the model was used to predict the residuary resistance based on hull geometry coefficients and the Froude number.

2) Dataset 2: Wine Quality [16]

Wine certification is an essential link to assure the quality of the wine market. The quality evaluation is often part of the certification process and can be used to improve winemaking and to stratify wines such as premium brands. The dataset is considered, with a total of 4898 white samples. Attribute information includes eleven physicochemical data of wines and quality evaluation from wine taster. In this test, the model was used to predict white wine quality based on physicochemical data.

3) Dataset 3: Behavior of the urban traffic of the city of Sao Paulo in Brazil [17]

The prediction of the traffic behavior could help to make a decision about the routing process. The database was created with records of behavior of the urban traffic of the city of Sao Paulo in Brazil from December 14, 2009, to December 18, 2009 (From Monday to Friday), with a total of 135 samples. Attribute information includes seventeen behavior of urban traffic and slowness in traffic (%). In this test, the model was used to predict slowness in traffic based on the behavior of urban traffic.

4) Dataset 4: Stock portfolio performance [18]

The return of investment portfolios can be increased by adopting the appropriate factors in stock. The database includes six weights of stock-picking concepts and six performances of portfolios with 315 samples from US stock market historical data. In this test, the model was used to predict the relative winning rate based on the weights of stock-picking concepts.

5) Dataset 5: Real estate valuation [19]

The market historical data set of real estate valuation is collected from Sindian Dist., New Taipei City, Taiwan, with 414 samples. Attribute information includes house price of the unit area and six attribute variables of house, such as the transaction date, the house age, and the distance to the nearest MRT station. In this test, the model was used to predict the house price of the unit area based on the attribute variables of houses.

6) Dataset 6: QSAR fish toxicity [20]

To prove that products are safe for both human health and the environment, REACH requires the evaluation of the short-term toxic effects on fish for substances imported or manufactured in quantities greater than 10 tonnes per year. The dataset is acute aquatic toxicity towards the fish *Pimephales promelas* (fat-head minnow) on a set of 908 chemicals. In this test, the model was used to predict LC50 data that is the concentration that causes death in 50

7) Dataset 7: Auto MPG [15,21]

This dataset is a slightly modified version of the dataset provided in the StatLib library. The data concerns city-cycle fuel consumption in miles per gallon, to be predicted in terms of three multivalued discrete and five continuous attributes [22]. In this paper, we removed a few samples that include unknown values and remained 392 samples. The model was used to predict mpg.

8) Dataset 8: Forest Fires [15]

Forest fires are a major environmental issue, creating economic and ecological damage while endangering human lives. The dataset includes twelve meteorological attributes and the burned area of the forest, with 517 samples. In this test, the model was applied to predict the burned area of the forest using meteorological data.

9) Dataset 9: Daily Demand Orders [23]

The dataset was collected a real database of a Brazilian logistics company for 60 days. The data has twelve predictive attributes and a target that is the total of orders for daily treatment.

10) Dataset 10: Concrete Compressive Strength [24]

Concrete is an essential material in civil engineering. The dataset includes eight concrete attributes and concrete compressive strength, with 1030 samples.

In this test, the model was applied to predict the concrete compressive strength.

5.1 Generalization capability

In practice, many vital factors potentially influenced the test results of generalization capability for an algorithm and were critical to consider in our analyses. Here are some factors we try best to consider: Firstly, for typical ANN, these factors may include the number of neurons in the hidden layer, initial weight values, activation function, and the network learning termination condition. Secondly, for CR-PNN, these factors are the number of layers and the network learning termination condition. Last but not least, in the aspect of data, these factors maybe are the division of data, the number of training samples, and the distribution of the dataset itself.

To be as comprehensive as possible, first of all, we tested the typical ANN ten times to adjust training parameters for each dataset. We found the typical ANN had better generalization capability for these datasets we obtained when the number of neurons in the hidden layer was 10. Besides, the network learning termination condition is to reach the preset training error (0.0001), training times (5000), or validation checks (6).

In this paper, we aimed to explore as many factors about data as possible impact on generalization capability, such as the impact of the number of training samples. Thus, we did not select cross-validation test methods used in previous literature (i.e., 5-fold cross-validation, 10-fold cross-validation or jackknife cross-validation test), and took the following exhaustive approach under guarantees of independent dataset test [25]:

Algorithm 1: CR-PNN .vs typical ANN

Input: Dataset
Output: MSE

```

1 for  $i = 1$  to 100 do
2   for  $n = t$  to end with  $c$  interval do
3     Randomly choose  $n$  samples from Dataset as the training samples;
4     Choose residual data as the testing samples;
5     Train CR-PNN;
6     Train typical ANN;
7     Test CR-PNN;
8     Test typical ANN;
```

We compare typical ANN and CR-PNN on various datasets, finding in all cases that CR-PNN gave results at least as good as, and often better than, typical ANN (see Fig. 7, we converted the input and output data into normalized data $[-1, 1]$). To some extent, CR-PNN is morphologically similar to PR. However, the computational complexity of PR does increase exponentially with the polynomial order, and for this condition, CR-CNN requires only increasing one layer, whether the present layers are. Additionally, it has commonly been assumed that PR is prone to be overfitting, yet, CR-CNN overcomes this due to

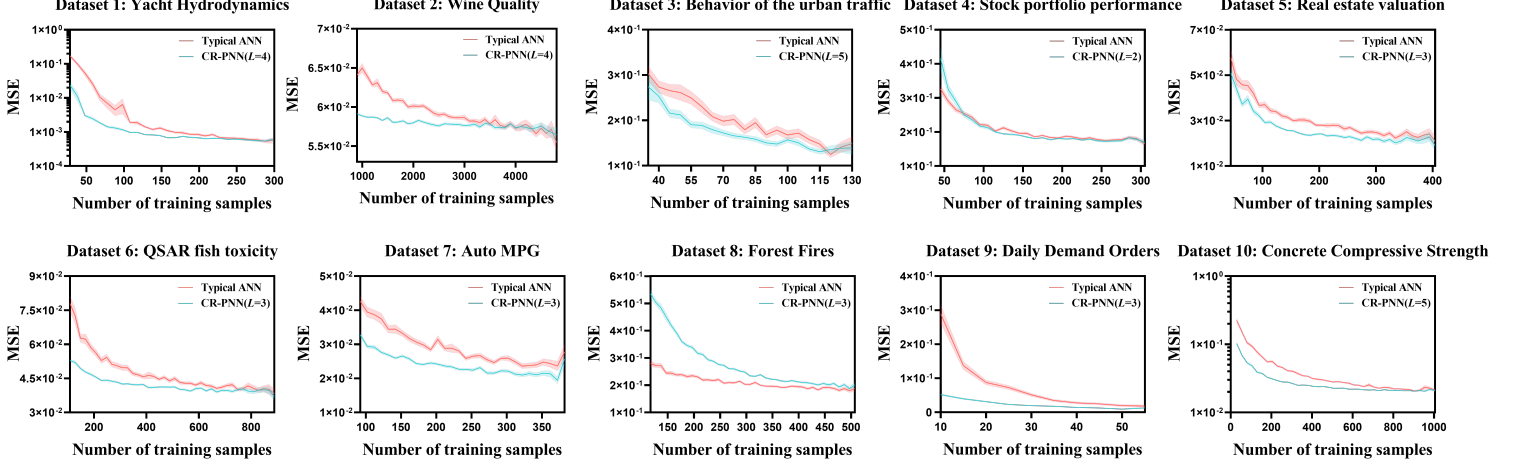


Figure 7: Compare results of generalization capability. All the networks for 100 runs. MSE: mean \pm SEM.

its structure and learning rules. Concretely, the gradual gradient decrease from the next layer to the former layer during error backward propagation because the absolute value of the input is normalized to $[-1, 1]$. Also, the weight of the higher layer of CR-PNN has a more significant impact on the lower items coefficients. Thus, CR-CNN firstly fits the outline of output space by lower item, and later the higher item with small values modifies the details. Ideally, the highest item is infinitesimal. This phenomenon is similar to Taylor expansion.

In addition, the existing ANNs are also, in fact, essentially PR [8]. Some connections between ANNs and polynomials have been noted in the literature [5, 8, 26]. Because the typical ANNs look like a black-box, we have to adjust the hyperparameters over and over. The transparent CR-PNN seems to easily get the model with great generalization capability more easily.

5.2 Computational complexity

The operation of CR-PNN only uses matrix multiplication and hadamard product, and it is well known that the computational complexity of hadamard product is significantly lower than nonlinear functions. Thus, the computational complexity of CR-PNN may be far lower than typical ANNs. To validate this conjecture, we designed two experiments about network training and application in real-time. For network training, multiple factors influence the running times of network training, such as learning rate and the termination condition. To eliminate the effects of other factors and focus on the network itself, we test the running time of typical ANN and CR-PNN for 1000 epoch with 4898 samples from Wine Quality Dataset (it has 11 input and one output). One epoch

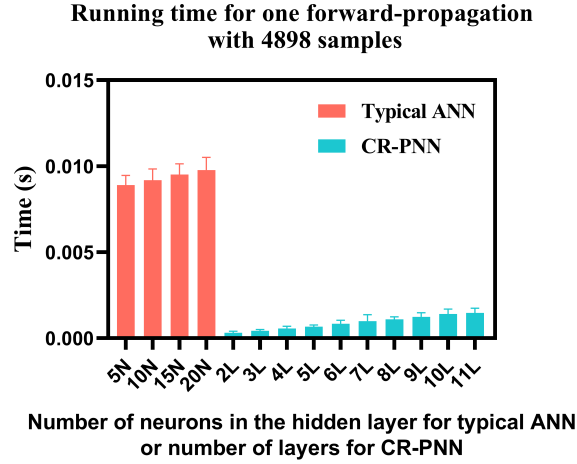
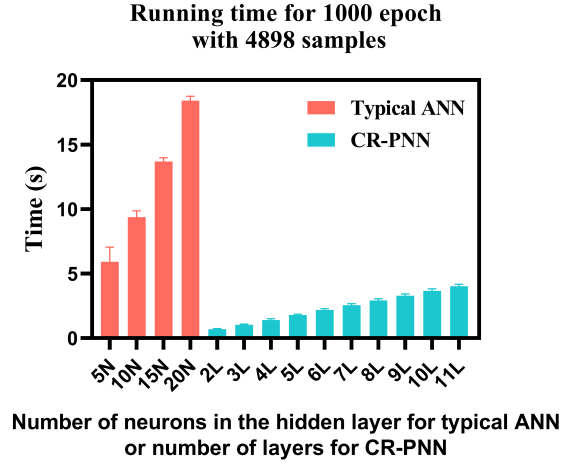


Figure 8: Comparison results of computational complexity. number N expresses a typical ANN with number neurons in hidden layer . number L expresses a CR-PNN with number layers. Additionally, as a example, we selected tansig as the activation function in hidden layer of typical ANN. All the networks for 200 runs.

is one forward-propagation plus one error-backpropagation for 4898 samples. In the aspect of an application in real-time, we test the running time of typical ANN and CR-PNN for one forward-propagation with 4898 samples. Both experiments repeatedly run 200 times using different parameter networks, as shown in Fig. 8. As we expected, the time complexity of CR-PNN is far lower than typical ANN, whether one epoch or one forward-propagation.

5.3 Notes and small skills

1) The diagonal matrix can be selected as the initialization weight matrix, and the initialization weight should be as small as possible. 2) The input and output are best normalized to $[-1, 1]$. 3) When the network is upgraded, the network weights can be initialized using the trained low-order network weights. The recommended strategy is to gradually increase the network order for training as the method indicated in Reference [27] (see Fig. 9).

6 Conclusion

In this paper, we consider that ANNs look like a black-box which makes the analysis of system and adjustment of the hyperparameters highly inconvenient. Inspired by Taylor expansion, a novel polynomial neural network is proposed to tackle this problem. The network is simple enough to be described as one small formula. The network firstly fits the outline of output space by lower item, and later the higher item with small values modifies the details. Ideally, the highest item is infinitesimal. Extensive simulations and real-world datasets obtained from different fields are used to explore the property of CR-PNN. Here, we show the following attractive property:

1) The internal structure of the network can be explained, which is of great use for system identification.

2) The result of CR-RNN happens to be a Taylor expansion and converges to Maclaurin series. We can achieve targeted control of precision when we tune the hyperparameters. Additionally, the network maybe is useful tools to solve the Taylor expansion for functions that cannot be represented by the formula.

3) In some cases, benefit from the structure and learning rules, the generalization capability of CR-RNN matches, and often exceeds that of typical ANNs.

4) Although the result of CR-PNN is morphologically similar to PR, CR-PNN overcomes that the computational complexity does increase exponentially with the polynomial order. CR-PNN only increase one layer to increase a order no matter how many the present layers are. Additionally, the complexity of CR-PNN is far lower than typical ANNs in the same effect.

Before ending this paper, it is worth mentioning that, to the best of our knowledge, this is the first neural network which determines the polynomial coefficients term by term from lower to higher degree due to learning rules that imitates the approximation order of Taylor expansion.

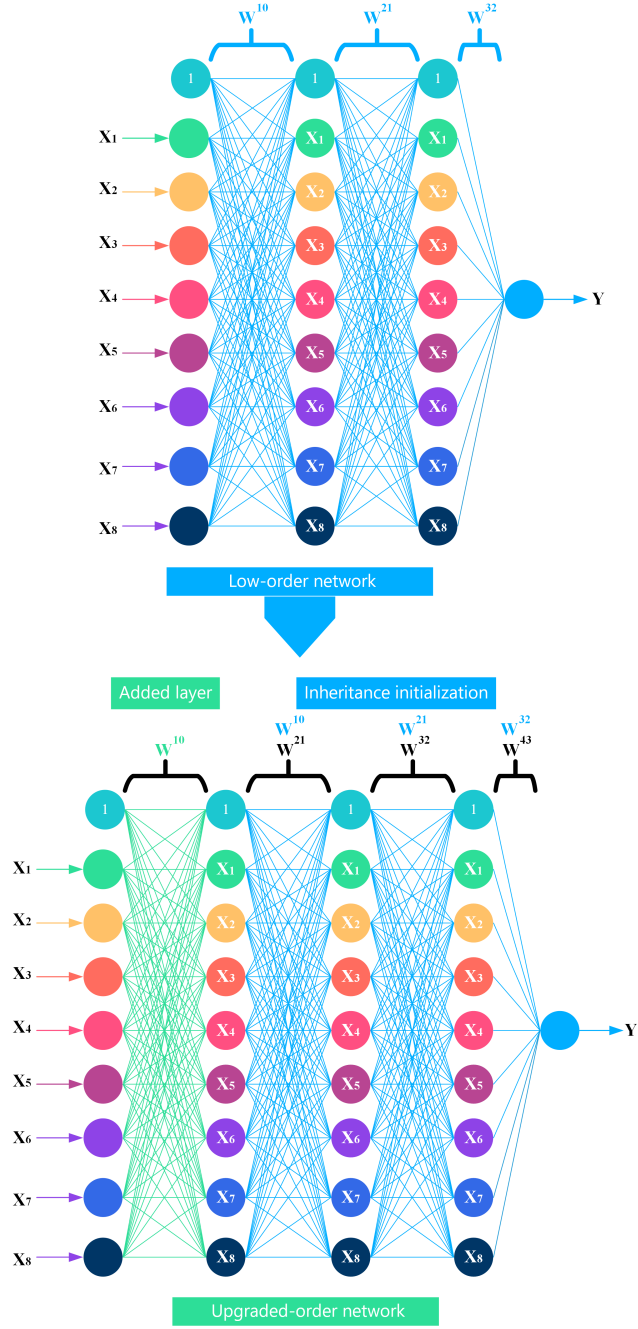


Figure 9: Example of inheritance initialization. The weight matrix of added layer is initialized to diagonal matrix with equal element values.

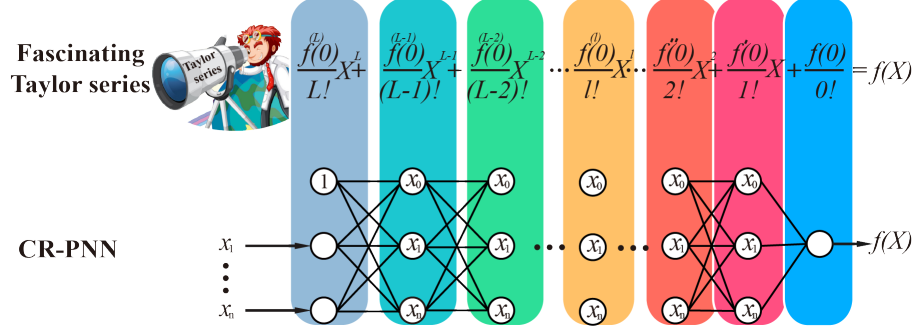


Figure 10: CR-PNN.

ACKNOWLEDGMENT

The authors would like to thank Andrew Ng for deep learning videos inspiring this work.

References

- [1] S. C. Gao, M. C. Zhou, Y. R. Wang, J. J. Cheng, H. Yachi, and J. H. Wang. Dendritic neuron model with effective learning algorithms for classification, approximation, and prediction. *Ieee Transactions on Neural Networks and Learning Systems*, 30(2):601–614, 2019.
- [2] Y. P. Pan and H. Y. Yu. Biomimetic hybrid feedback feedforward neural-network learning control. *Ieee Transactions on Neural Networks and Learning Systems*, 28(6):1481–1487, 2017.
- [3] S. Li, H. Q. Wang, and M. U. Raffique. A novel recurrent neural network for manipulator control with improved noise tolerance. *Ieee Transactions on Neural Networks and Learning Systems*, 29(5):1908–1918, 2018.
- [4] Kurt Hornik, Maxwell B Stinchcombe, and Halbert White. Multilayer feed-forward networks are universal approximators. *Neural Networks*, 2(5):359–366, 1989.
- [5] Rich Caruana, Steve Lawrence, and C Lee Giles. Overfitting in neural nets: Backpropagation, conjugate gradient, and early stopping. In *Advances in neural information processing systems*, pages 402–408, 2001.
- [6] F. Yu and X. Z. Xu. A short-term load forecasting model of natural gas based on optimized genetic algorithm and improved bp neural network. *Applied Energy*, 134:102–113, 2014.

- [7] S. Kirkpatrick, C. D. Gelatt, and M. P. Vecchi. Optimization by simulated annealing. *Science*, 220(4598):671–680, 1983.
- [8] Cheng Xi, B. Khomtchouk, N. Matloff, and P. Mohanty. Polynomial regression as an alternative to neural nets. *arXiv*, pages 28 pp.–28 pp., 2018.
- [9] T. Poggio. On optimal nonlinear associative recall. *Biological Cybernetics*, 19(4):201–209, 1975.
- [10] Alex Krizhevsky, Ilya Sutskever, and Geoffrey E Hinton. Imagenet classification with deep convolutional neural networks. In *Advances in neural information processing systems*, pages 1097–1105, 2012.
- [11] D. E. Rumelhart, G. E. Hinton, and R. J. Williams. Learning representations by back-propagating errors. *Nature*, 323(6088):533–536, 1986.
- [12] J. Sjöberg, Q. H. Zhang, L. Ljung, A. Benveniste, B. Delyon, P. Y. Glorennec, H. Hjalmarsson, and A. Juditsky. Nonlinear black-box modeling in system identification: A unified overview. *Automatica*, 31(12):1691–1724, 1995.
- [13] G. Cybenko. Approximation by superpositions of a sigmoidal function. *Mathematics of Control, Signals, and Systems*, 2(4):303–314, 1989.
- [14] G. Y. Chen, M. Gan, F. Ding, and C. L. P. Chen. Modified gram-schmidt method-based variable projection algorithm for separable nonlinear models. *Ieee Transactions on Neural Networks and Learning Systems*, 30(8):2410–2418, 2019.
- [15] Paulo Cortez and Aníbal de Jesus Raimundo Morais. A data mining approach to predict forest fires using meteorological data. 2007.
- [16] P. Cortez, A. Cerdeira, F. Almeida, T. Matos, and J. Reis. Modeling wine preferences by data mining from physicochemical properties. *Decision Support Systems*, 47(4):547–553, 2009.
- [17] Carlos Affonso, Renato José Sassi, and Ricardo P Ferreira. Traffic flow breakdown prediction using feature reduction through rough-neuro fuzzy networks. In *The 2011 International Joint Conference on Neural Networks*, pages 1943–1947. IEEE, 2011.
- [18] Yicheng Liu and Icheng Yeh. Using mixture design and neural networks to build stock selection decision support systems. *Neural Computing and Applications*, 28(3):521–535, 2017.
- [19] I. C. Yeh and T. K. Hsu. Building real estate valuation models with comparative approach through case-based reasoning. *Applied Soft Computing*, 65:260–271, 2018.

- [20] M. Cassotti, D. Ballabio, R. Todeschini, and V. Consonni. A similarity-based qsar model for predicting acute toxicity towards the fathead minnow (*pimephales promelas*). *Sar and Qsar in Environmental Research*, 26(3):217–243, 2015.
- [21] Dheeru Dua and Casey Graff. A data mining approach to predict forest fires using meteorological data, 2017.
- [22] J Ross Quinlan. Combining instance-based and model-based learning. In *Proceedings of the tenth international conference on machine learning*, pages 236–243, 1993.
- [23] Ricardo Pinto Ferreira, Andrea Martiniano, Arthur Ferreira, Aleister Ferreira, and Renato Jose Sassi. Study on daily demand forecasting orders using artificial neural network. *IEEE Latin America Transactions*, 14(3):1519–1525, 2016.
- [24] I. C. Yeh. Modeling of strength of high-performance concrete using artificial neural networks. *Cement and Concrete Research*, 28(12):1797–1808, 1998.
- [25] J. D. Rodriguez, A. Perez, and J. A. Lozano. Sensitivity analysis of k-fold cross validation in prediction error estimation. *Ieee Transactions on Pattern Analysis and Machine Intelligence*, 32(3):569–575, 2010.
- [26] Sung-Kwun Oh, Witold Pedrycz, and Byoung-Jun Park. Polynomial neural networks architecture: analysis and design. *Computers & Electrical Engineering*, 29(6):703–725, 2003.
- [27] Geoffrey E Hinton, Simon Osindero, and Yee Whye Teh. A fast learning algorithm for deep belief nets. *Neural Computation*, 18(7):1527–1554, 2006.